Phys. Status Solidi B **247**, No. 8, 2084–2088 (2010) / **DOI** 10.1002/pssb.200983928

physica status solidi b
www.pss-b.com
basic solid state physics

Spectrally dependent locations of hot-spots in nanoparticle clusters

Paul Anton Letnes* **and Ingve Simonsen**

Department of Physics, Norwegian University of Science and Technology (NTNU), NO-7491, Trondheim, Norway

Received 14 December 2009, revised 20 January 2010, accepted 24 February 2010
Published online 14 June 2010

Keywords clusters, dielectric functions, electrostatics, nanoparticles

* Corresponding author: e-mail paul.anton.letnes@gmail.com, Phone: +47 98 62 08 26, Fax: +47 735 97 710

We study the optical response of clusters of metallic nanospheres in the electrostatic approximation, using a spherical harmonic representation of the electric field. Field enhancement and near field interactions between the spheres are investigated numerically. Symmetry properties of certain clusters give rise to highly localized maxima of the electric field, denoted "hot spots." From numerical experiments performed at optical frequencies of the incident light, it is found that various geometrical configurations exhibit interesting phenomena; in particular, that hot spots move spatially around as a function of the frequency of the incident light. We present simulation results for the simplest nanoparticle cluster known to exhibit these interesting phenomena, namely, a regular octahedron.

1 Introduction At least since the time of the Romans, the pronounced optical effects of metallic nanoparticles has been taken advantage of for producing vibrant color effects in, e.g., glass [1]. However, it was first many years later that this phenomenon was fully understood. By the rigorous electromagnetic scattering theory for a spherical particle developed by Mie [2] more than a hundred years ago, it was fully realized that the highly frequency dependent optical response of subwavelength metallic particles is caused by the so-called *plasmon resonances* [3–5]. These resonances can be excited by incoming light under the right conditions, e.g., evanescent fields impinging on a surface.

Since Mie's seminal work, uncountable experimental, theoretical and numerical electromagnetic studies have been performed on systems consisting of nanoparticles. Today, such systems find applications in numerous branches of technology and science, such as detecting adsorption of biological substances on surfaces, optical antennae, and surface enhanced Raman scattering (SERS) experiments.

A new wave of interest in the optical properties of subwavelength metallic particles came with the discovery of the SERS phenomenon more than 30 years ago [6]. In these studies it was reported that the Raman signal from a given type of molecules was enhanced by about six orders of magnitude when the molecules were adsorbed on the surfaces of small metal particles or on rough metal surfaces. Such levels of enhancements are today commonly attributed to the excitation of localized surface plasmon resonances in the metal.

More recently, Raman enhancements[1] as high as 14 orders of magnitude have been reported in the literature for *clusters* of particles [7]. Moreover, it is so far reported for certain cluster geometries that enhancements of 9–11 orders of magnitude can be attributed to surface plasmon excitations in the cluster. This is orders of magnitude more than what is possible to achieve with a single particle [8].

In the past, experimentalists have traditionally used colloidal nanoparticles for field enhancement studies. However, with the advent of various technologies for creating nanoscopic structures, this has changed, since it now has become practically feasible to manipulate objects on the nanoscale with confidence. This has opened for the possibility of *engineering* clusters of well-defined geometry and/or particle shapes to be used for large field enhancement studies. These fascinating possibilities have initiated a lot of theoretical and numerical studies into the properties of more complex clusters of nanoparticles [8–12], various particle shapes [13–15] as well as supported nanoparticles [5, 15–18].

[1] The Raman cross-section scales as the 4th power of the local electric field.

It is worth noting that the field is not enhanced uniformly within a cluster. Instead one has regions of field enhancement, so-called "hot spots," where the local field enhancement is particularly high. In the past, "simpler" cluster geometries have been considered, typically linear geometries like dimers and nanoparticle chains [8–12] for which the location of the hot spots can be inferred from theory. However, for more complicated two- or three-dimensional structures, the hot spot locations are not known in advance.

This paper is devoted to the study of clusters of spherical nanoparticles, where we report results for a 3D "double pyramid" geometry (octahedron). The locations of the hot spots for this geometry are presented for optical frequencies. The main result of the paper is that the locations of the hot spots are frequency dependent: observed hot spots *move around spatially* in a priori unpredictable ways, as the frequency of the incident light changes. To the best of our knowledge, such results have not been reported previously.

2 Geometry The physical system we consider in this work consists of $N = 6$ dielectric spheres of radii R_i $(i = 1, 2, \ldots, 6)$ and dielectric functions $\varepsilon_i(\omega)$ surrounded by a medium characterized by a (non-absorbing) dielectric function $\varepsilon_0(\omega)$. The spheres are arranged in an *octahedron* geometry with its center located at the origin of a coordinate system (x, y, z). Four of the sphere centers are situated in the yz-plane at positions $(0, \pm\ell, \pm\ell)$ and $(0, \pm\ell, \mp\ell)$ where ℓ is a length scale to be specified. The remaining two spheres are located on the x-axis at $x = \pm\sqrt{2}\ell$. The full geometry of the cluster of spherical particles we are concerned with is depicted in Fig. 1. This particular geometry is discussed because it is the simplest geometry known to exhibit spectrally dependent hot-spot locations.

In addition to the coordinate system, $\mathcal{S}$, centered at the center of the octahedron, we also introduce $N = 6$ coordinate systems, $\mathcal{S}_i$, with spherical coordinates (r_i, θ_i, ϕ_i) and with their origins located at the center of sphere i, related to $\mathcal{S}$ by pure translation.

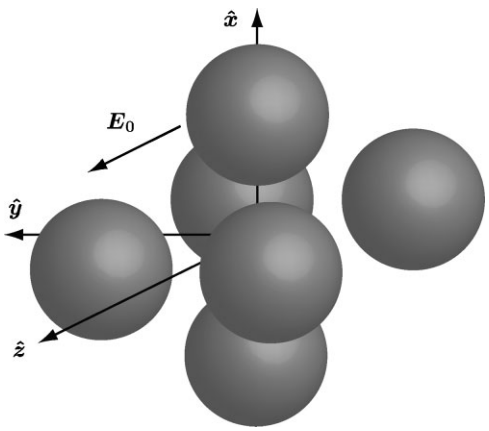

Figure 1 The regular octahedron nanosphere cluster with four spheres in the yz plane and two spheres on the x axis. $\boldsymbol{E}_0$ is uniform and oriented along the z axis.

For the purpose of this work, we will assume that all spheres are identical, and therefore share the same radius, $R_i \equiv R$. The material of all spheres is chosen to be silver and the experimental data for the dielectric function $\varepsilon_i(\omega) \equiv \varepsilon(\omega)$ is taken from the SOPRA database [19]. The incident electric field is set to $\boldsymbol{E}_0 = \hat{z}E_0$, and we choose the length scale ℓ to be $\ell = 1.1R$.

3 Theory It will be assumed that the size of the cluster of spheres is much smaller than the wavelength, i.e., $2\sqrt{2}\ell \ll \lambda$. Hence, the whole system under study is therefore much smaller than the wavelength of the incident radiation. Under this assumption, one can work within the so-called quasi-static approximation, for which all retardation effects can be neglected. In this case, it is well known that the Maxwell's equations are consistent with solving the Laplace equation,

$$\nabla^2\psi(\boldsymbol{r}) = 0, \tag{1}$$

satisfied by the scalar potential, $\psi(\boldsymbol{r})$, given appropriate boundary conditions [20, 21]. Once the potential is known, the related electric field is obtained from $\boldsymbol{E}(\boldsymbol{r}) = -\nabla\psi(r)$. The boundary conditions to be satisfied by the potential at any interface separating media of different dielectric properties follow from the corresponding boundary conditions for the electric field. This translates into the requirement that the potential $\psi(\boldsymbol{r})$ itself and its normal derivative $(\partial_n = \hat{n}\cdot\nabla)$ times the dielectric function of the medium where the potential is being calculated, $\varepsilon(\omega)\partial_n\psi(\boldsymbol{r})$, should both be *continuous* over any interface separating two adjacent media.

In a spherical geometry, a general solution to the Laplace equation is known in terms of the so-called multipole expansion. It consists of a series expansion in terms of positive (r^l) and negative (r^{-l-1}) powers of the distance, r, from the origin of the coordinate system times the spherical harmonics, $Y_l^m(\theta, \phi)$, which take care of the angular dependence of the potential [5, 20, 21]. In order to keep the potential finite everywhere, expansion coefficients for terms like r^{-l-1} must be put to zero for the domain containing the origin of the coordinate system. For the same reason, terms containing positive powers of r are not allowed in domains extending to infinity, i.e., outside the spheres.

For our cluster of spherical particles, the procedure is now to expand the potential in the local systems S_j of spherical coordinates (r_j, θ_j, ϕ_j) and having its origin at the center of sphere j as follows (with the shorthand $\sum_{lm} \equiv \sum_{l=0}^{\infty}\sum_{m=-l}^{l}$):

$$\psi_j(\boldsymbol{r}_j) = \begin{cases} \sum\limits_{lm} A_{lm}^{(j)} \left(\frac{r_j}{R}\right)^{-l-1} Y_l^m(\theta_j, \phi_j), & \text{if } r_j > R, \\ \sum\limits_{lm} B_{lm}^{(j)} \left(\frac{r_j}{R}\right)^{l} Y_l^m(\theta_j, \phi_j), & \text{if } r_j \le R. \end{cases}$$

In the embedding medium, and therefore outside all spheres, the (total) potential can be written in the form

$$\psi(\boldsymbol{r}) = -\boldsymbol{r}\cdot\boldsymbol{E}_0 + \sum_{j=1}^{N}\psi_j(\boldsymbol{r}_j). \tag{2}$$

Here the first term stems from the incident field, which for simplicity has here been taken to be constant and uniform, while the second term is the contributions to the potential from the individual spheres. To facilitate the matching of boundary conditions on the spherical interface, we express $\boldsymbol{r}\cdot\boldsymbol{E}_0$ in terms of Y_1^0 and $Y_1^{\pm 1}$ [5].

The coefficients $A_{lm}^{(j)}$ and $B_{lm}^{(j)}$ appearing in the expansions for ψ_j are all unknown, but they are determined by imposing the appropriate boundary conditions for the potential on the surface of each of the $N = 6$ spheres. However, one problem arises when one wants to do this: Eq. (2) involves coordinates from $N+1$ different systems, and $\{_j\}_{j=1}^{N}$, but they are all related to each other via the position vectors of the centers of the various spheres. Here the so-called translation addition theorem for spherical harmonics comes to our rescue [5]. What this theorem says is that under certain conditions (that are satisfied here) the various terms of the multipole expansion given in terms of one coordinate system, say, $r^{-l-1}Y_l^m(\theta_j,\phi_j)$ can be expressed, with *known* expansion coefficients, as a linear combination of $r^{l'}Y_{l'}^{m'}(\theta_i,\phi_i)$ from another coordinate system ($i \neq j$) with $l' \leq l$ and, as usual, $|m'| \leq l'$ (see Ref. [5] for details). This implies that all the potentials going into satisfying the boundary conditions at the surface of a given sphere can, for instance, be expressed in terms of the coordinates associated with that sphere alone. Taking into account all the boundary conditions on the surface of the spheres and using the orthogonality of the spherical harmonics, a set of linear equations can be derived for the expansion coefficients $A_{lm}^{(j)}$ and $B_{lm}^{(j)}$. Moreover, it can be shown that the $B_{lm}^{(j)}$ coefficients, related to the potentials inside the sphere, can be eliminated from the linear system of equations thereby leaving only $A_{lm}^{(j)}$. Furthermore, it follows from the continuity of $\varepsilon\partial_n\psi$ that $A_{00}^{(j)} = 0$. In practice the multipole expansion given above has to be truncated at, say, $l \leq L$ in order to give a finite size for the resulting linear system to be solved. Then the total number of unknown coefficients to be solved for is $N(L+1)^2 - 1$. After having determined the expansion coefficients, one can calculate $\psi(\boldsymbol{r})$ at any given point in space, and, subsequently, $\boldsymbol{E}(\boldsymbol{r})$, by numerical differentiation (using a finite difference approximation). We stress that this approach takes all particle–particle interactions into account.

4 Results We have performed numerical simulations for a nanooctahedron cluster consisting of $N = 6$ silver particles (Section 2) for photon energies in the range from 2.0 eV to 4.5 eV. The simulations were done under the quasi-static approximation, where the potential is expressed as a multipole expansion with $L = 20$ (Section 3). We have especially investigated how the locations of regions of high field enhancements, so-called "hot spots," depend on frequency. As we shall see, these hot spot regions tend to move around as we vary the frequency of the incident light.

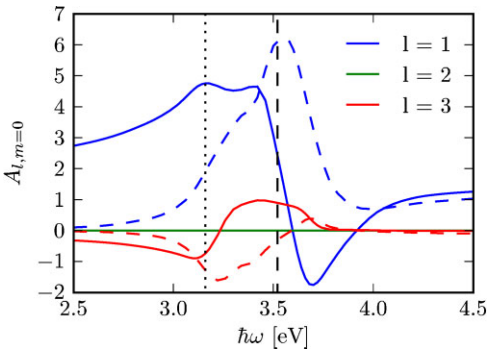

Figure 2 (online color at: www.pss-b.com) Frequency dependence of the expansion coefficients A_{l0} for the top sphere in Fig. 1. Solid and dashed lines show the real and imaginary parts of the coefficient, respectively. It is noted that *all even* multipole coefficients are identically zero (also those for $l > 3$ that are not shown). The dashed line represents the single-sphere Mie resonance, and the dotted line represents the red-shifted Mie resonance for interacting spheres.

In Fig. 2, the frequency dependence of the three lowest order multipole coefficients are presented for the silver $N = 6$ nanoparticle cluster under study. Solid and dashed lines give the real and imaginary parts of the expansion coefficients, respectively. Our first observation is that all terms with $m = 0$ and l even, in particular $l = 2$, $m = 0$, vanish for all frequencies. We explain this effect following closely the argument put forward in Ref. [12]: with the given field orientation, the electrostatic potential has to be antisymmetric with respect to reflection in the yz plane. As spherical harmonics gain a factor $(-1)^{l+m}$ under reflection through the xy plane, we expect that all coefficients A_{lm} with $l+m$ even will be zero, due to this symmetry constraint on the potential. Our hypothesis has been confirmed by simulating a regular octahedron cluster with the material of one sphere changed from silver to gold; this breaks the symmetry, and thus the selection rule for the l, m multipoles. In this case, all multipoles contribute (are non-zero), also the multipoles with $l+m$ even.

Another eye-catching feature of Fig. 2 is that for photon energies just above 3.5 eV, the real part of the dipole coefficient, A_{10}, vanishes, while the octupole term dominates. This indicates that for these intermediate frequencies, any field enhancement hot spots encircling the sphere in question will move around due to the different angular dependence of dipole and octupole terms. This, combined with the rapid oscillations (with respect to θ, ϕ) and the spatial decay (r^{-l-1}) of the high order multipoles, shows that these structures exhibit characteristics interesting for nanoantenna applications: creating a localized near field response under the influence of an incoming far field, with a frequency dependent position of the field enhancement.

Figures 3 and 4 show the field enhancement at $\hbar\omega = 3.5$ eV in the xz and xy planes, respectively, with the incident field $\boldsymbol{E}_0$ as indicated. In both planes we observe

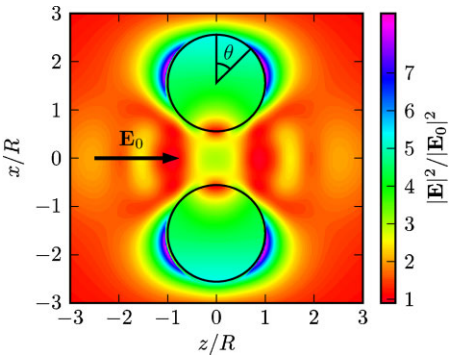

Figure 3 (online color at: www.pss-b.com) Normalized field enhancement $|\boldsymbol{E}|^2/|\boldsymbol{E}_0|^2$ in the xz plane, for an incident field of $\hbar\omega = 3.5$ eV. The two black circles indicate the circumference of the top and bottom spheres in Fig. 1, whose centers reside in the xz plane, while the four remaining spheres are entirely above or below the xz plane.

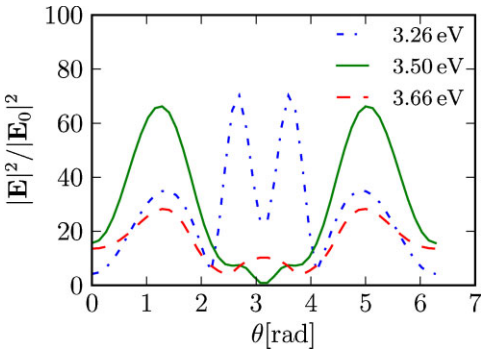

Figure 5 (online color at: www.pss-b.com) Intensity enhancement $|\boldsymbol{E}|^2/|\boldsymbol{E}_0|^2$ on the top black circle (i.e., the intersection between the surface of the sphere and the xz plane) for three different frequencies. Note that the peaks in the intensity enhancement do not coincide for all frequencies. θ is the angle shown in Fig. 3.

significant field enhancement hot spots at various locations, tied closely to the surfaces of the spheres. Intuitively, one expects the maximum field enhancement to occur where the spheres are closest. Although this holds true for some frequency ranges, i.e., where the dipole terms in our expansion dominate, it certainly does not hold true for all frequencies. For example, at $\hbar\omega = 3.50$ eV, as depicted in Fig. 3, we notice that the hot spots in the xz plane are located on the *outside* of our sphere cluster, near the top and bottom of the figure.

While Fig. 3 gives a good picture of what happens at one particular frequency, it is by nature unable to reveal any spectral dependencies. Figure 5 shows the intensity enhancement on the top black circle in Fig. 3, i.e., on the circle corresponding to the intersection between the xz plane and the sphere's surface. By changing the photon energy of the incident light from 3.26 eV to 3.50 eV, we observe that the two peaks close to $\theta = \pi$ are significantly reduced, while the side peaks close to $\theta = \pm\pi/2$ grow in strength. Increasing the photon energy up to 3.68 eV, the pattern changes completely, showing only three peaks in the field enhancement.

Figure 6 shows the field enhancement for a range of photon energies, revealing in more detail the behavior of the field enhancement peaks. According to the figure, peaks of field enhancement appear and disappear in several locations at different frequencies, indicating that the most important effect is the appearance and disappearance of hot spots at static locations.

Figure 7, included for completeness, shows the same as Fig. 6, but now in the xy plane, with the different θ values corresponding to different locations on the top black circle in Fig. 4. Interestingly, the two hot spots found at low photon energies vanish for energies of about 3.50 eV, while a new, broad resonance forms across most of the circumference in the xy plane.

While we in this paper have focused on one specific cluster of silver nanospheres, namely the regular octahedron, we have also simulated other cluster geometries. As an

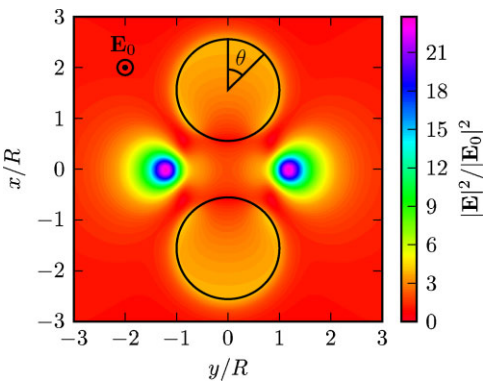

Figure 4 (online color at: www.pss-b.com) Field enhancement $|\boldsymbol{E}|^2/|\boldsymbol{E}_0|^2$ in the xy plane, at a frequency of $\hbar\omega = 3.5$ eV. The two black circles indicate the circumference of the top and bottom spheres in Fig. 1. The four remaining spheres are entirely above or below the xy plane.

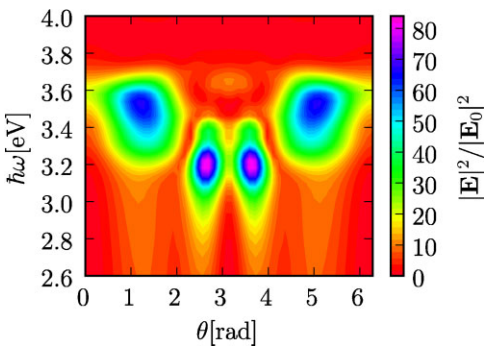

Figure 6 (online color at: www.pss-b.com) Intensity enhancement on the great circle in the xz plane (i.e., the intersection between the surface of the sphere and the xz plane), for the top sphere in Fig. 1. The angle, θ, is shown in Fig. 3. It is possible to recognize the four hot spots of the field from Fig. 3.

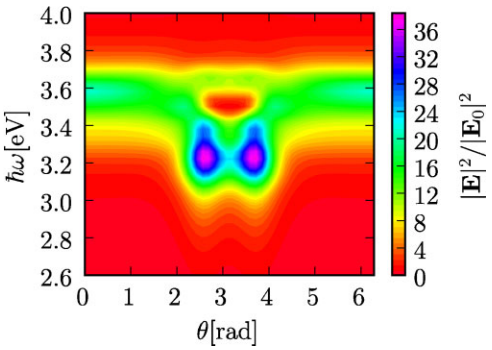

Figure 7 (online color at: www.pss-b.com) Intensity enhancement on the great circle in the *xy* plane, for the top sphere in Fig. 1. The angle, θ, is shown in Fig. 4.

example, we have calculated field enhancement inside a cluster consisting of spheres placed at the lattice points in a single FCC unit cell; the same was also done for a single BCC unit cell. In both cases, we observed wandering hot spots, indicating that this phenomenon is *robust*; i.e., it occurs for many different types of 3D clusters.

To ensure the validity of our numerical calculations, we investigated the convergence by explicitly verifying that the boundary conditions at each spherical interface were fulfilled. Using the truncation rule suggested in Ref. [9], $L = 4R/d = 20$, the observed errors were found to be less than 1%, which is satisfactory for a qualitative study.

5 Conclusion and outlook In conclusion, we have observed the spectral dependence of hot spot locations in clusters of nanospheres. Working in the quasi-static approximation, we show that the frequency dependence of the dielectric function alone is enough to provoke rich dynamics in the local electric field. The dielectric functions were taken from experiments, giving confidence in the possibility of observing such phenomena in real systems.

Interesting future work includes looking at (truncated) spheres placed on a planar interface, as this is a more convenient system to investigate experimentally. Using a similar approach to solve the Laplace equation seems feasible for such systems. Another possibility is to investigate if frequency dependent hot spots are observed in spheres coated by another dielectric.

Acknowledgements The authors thank Dr. Ola Hunderi, Dr. Douglas L. Mills and Tor Nordam for stimulating discussions. The research of I.S. was supported by Research Council of Norway under the program Småforsk and an NTNU Mobility Fellowship.

References

[1] F. E. Wagner, S. Haslbeck, L. Stievano, S. Calogero, Q. Pankhurst, and K. P. Martinek, Nature **407**, 691 (2000).
[2] G. Mie, Ann. Phys. (Leipzig) **25**, 330 (1908).
[3] C. Bohren and D. Human, Absorption and Scattering of Light by Small Particles (John Wiley & Sons, New York, 1983).
[4] H. van de Hulst, Light Scattering by Small Particles (Dover Publishing Company, New York, 1981).
[5] D. Bedeaux and J. Vlieger, Optical Properties of Surfaces, second edition (Imperial College Press, London, 2004).
[6] M. Moskovits, Rev. Mod. Phys. **57**, 783–826 (1985).
[7] S. Nie and S. Emory, Science **275**, 1102 (1997).
[8] C. Noguez, J. Phys. Chem. **111**, 3806 (2007).
[9] K. Li, M. I. Stockman, and D. J. Bergman, Phys. Rev. Lett. **91**, 227402 (2003).
[10] R. Arias and D. L. Mills, Phys. Rev. B **68**, 245420 (2003).
[11] K. Arya, Phys. Rev. B **74**, 195438 (2006).
[12] P. Chu and D. L. Mills, Phys. Rev. B **77**, 045416 (2008).
[13] J. Mock, M. Barbic, D. Smith, D. Schultz, and S. Schultz, J. Chem. Phys. **116**, 6755 (2002).
[14] J. Aizpurua, W. Garnett, L. Richter, and F. J. G. de Abajo, Phys. Rev. B **71**, 235420 (2005).
[15] R. Lazzari, I. Simonsen, D. Bedeaux, J. Vlieger, and J. Jupille, Eur. Phys. J. B **24**, 267 (2001).
[16] R. Lazzari, I. Simonsen, and J. Jupille, Europhys. Lett. **61**, 541 (2003).
[17] R. Lazzari, S. Roux, I. Simonsen, J. Jupille, B. Bedeaux, and J. Vlieger, Phys. Rev. B **65**, 235424 (2002).
[18] I. Simonsen, R. Lazzari, J. Jupille, and S. Roux, Phys. Rev. B **61**, 7722 (2000).
[19] http://www.sopra-sa.com/.
[20] J. Jackson, Classical Electrodynamics, third edition (John Wiley & Sons, New York, 2007).
[21] J. Stratton, Electromagnetic Theory, IEEE Press Series on Electromagnetic Wave Theory (Wiley-IEEE Press, New York, 2007).

